the Au 5d orbitals enough to produce AuI_3. $AgCl_2$, $AgBr_2$, and AgI_2 will also be favored by high pressure. For Hg^{II} compounds a reduction in Hg-L distance will lead to a reduced Hg 5d-L p separation and a stronger destabilization. Such destabilization could be reduced by disproportionation to Hg^{I} and Hg^{III}, both of which might have larger Hg 5d-L p separations than the original Hg^{II} compound. The above effects would occur whether the application of pressure lead to only a gradual reduction in M-L or to a transformation to a higher coordination number polymorph, since distance reduction and coordination number increase have similar effects upon M d orbital energies (so long as the initial coordination number is small).

Conclusion. Analysis of quantum mechanical calculations and X-ray spectra of binary compounds of Cu and Zn family metals indicates individual members differ significantly in M d-L p energy separation and the extent of M d-L p orbital mixing. For the heaviest members of the families, Au and Hg, the M d levels are raised significantly by relativistic effects. In addition to its dependence on metal and ligand identity, the M d-L p energy separation is strongly influenced by M coordination number resulting in significant differences in M d-L p separation between gaseous molecules and solids of the same stochiometry. It appears that many aspects of the structures of Cu and Zn family compounds can be understood on the basis of the following simple principles: (1) Ionic forces favor higher oxidation states. (2) An oxidation state is stable only if all unoccupied M d orbitals (if any) lie above the L p nonbonding orbitals in energy. (3) The average energies of M d orbitals are lowered 1-2 eV by a unit increase in oxidation state. (4) An oxidation state increase therefore decreases the M d-L p energy difference for Cu, increases it for Ag, Au, and Hg, and gives little percentage increase in its initially large value for Zln and Cd compounds. (5) Compounds with one empty or partially filled M d orbital will distort so as to destabilize this orbital, with the effect increasing as the M d-L p separation decreases. (6) Compounds with completely filled M d shells and small M d-L p energy differences will adopt structures whose coordination numbers yield maximum M d-L p energy differences and minimum M d-L p orbital mixing. For Cu compounds this effect will tend to favor large coordination numbers while for Au, Ag, and Hg low coordination numbers will be favored.

Acknowledgment. This work was supported by NASA, Grant No. NSG-7482, and NATO, Grant No. 1509. Computer costs were partly supported by the Computer Science Center, University of Maryland.

Registry No. ZnS_4^{6-}, 63915-41-3; CdS_4^{6-}, 78279-97-7; HgS_2^{2-}, 26015-93-0; HgS_4^{6-}, 78279-98-8; $ZnCl_4^{2-}$, 15201-05-5; $CdCl_6^{4-}$, 44433-10-5; $HgCl_2$, 7487-94-7; $HgCl_4^{2-}$, 14024-34-1; Cu_2S, 22205-45-4; Ag_2S, 21548-73-2; AgS_2^{3-}, 78279-99-9; AgS_4^{7-}, 78280-00-9; AuS_2^{3-}, 78280-01-0; CuCl, 7758-89-6; AgCl, 7783-90-6; $ZnCl_2$, 7646-85-7; $ZnCl_6^{4-}$, 63344-34-3.

Contribution from Bell Laboratories,
Murray Hill, New Jersey 07974

Excitation, Ionization, and Fragmentation in Dimethylmercury

A. GEDANKEN, M. B. ROBIN,* and N. A. KUEBLER

Received January 13, 1981

Unlike the situation in metal carbonyls where M^+ ions result from multiphoton ionization (MPI) of the photoproduced metal atoms, the MPI of $Hg(CH_3)_2$ proceeds through the parent molecular ion $Hg(CH_3)_2^+$ which then photofragments to yield Hg^+. This is demonstrated by the absence of Hg(I) atomic lines in the MPI spectrum and also by mass spectrometry wherein a considerable quantity of molecular parent ion is observed at low laser flux while at high flux this is replaced totally by Hg^+. The MPI spectrum of $Hg(CH_3)_2$ in a jet-cooled, seeded molecular beam displays a two-photon-allowed/one-photon-forbidden Rydberg excitation ($A_1' \rightarrow E''$) in the 51 000-56 000 cm^{-1} region. The Jahn-Teller splitting (14 cm^{-1}) of the $\nu_{11}(1,1)$ sequence bands in the upper state of this transition confirms its E'' spin-orbit assignment. Clustering in the beam removes the sharp-line MPI features totally, as appropriate for a Rydberg excitation. The inelastic electron-impact spectrum of $Hg(CH_3)_2$ also was recorded up to 30-eV loss, and the transitions were assigned with due regard for the strong spin-orbit splitting within the one-electron configurations and the Rydberg term-value concept.

Pulsed-laser irradiation of several transition-metal carbonyls recently has uncovered some rather unexpected results.[1-3] In particular, though the one-photon electronic spectra of the transition-metal carbonyls are generally so broad that no vibrational structure is discernible, the same compounds when studied by the multiphoton ionization (MPI) spectroscopic technique[4] yield a tremendous number of very sharp lines. As shown by Vaida et al.[2,5] these lines are due to MPI processes in the bare metal atom, and, indeed, the MPI mass spectra are strongly dominated by the presence of M^+ ions formed by photoionization.[1,3] On the other hand, $M(CO)_6^+$, $M(CO)_5^+$, ..., etc. are abundant in the electron-impact mass spectra of the same materials.[6] By way of explanation, it appears that the first two photons are absorbed coherently in the transition-metal carbonyls, followed by a rapid loss of CO ($>10^{12}$ s^{-1}) in this and in subsequent incoherent absorption steps. Even though enough energy is pumped into the molecular system to ionize it, the competing dissociation to M + 6CO is overwhelmingly the favored path kinetically, and only M^+ ions form on further absorption of light. Using 3546-Å laser pulses (3546 Å = 3.496 eV) and a time-of-flight mass spectrometer, we have observed only monoatomic M^+ ions when irradiating $Cr(CO)_6$ (17.07 eV), $Mo(CO)_6$ (19.63), $W(CO)_6$ (22.25), $V(CO)_6$ (15.5), $Fe_2(CO)_9$, $Mn_2(CO)_{10}$ (22.13), and $Co_2(CO)_8$ (16.9). The M^+ appearance potentials[7] are given in parentheses. Most recently, this metal-ion-only effect has been

(1) M. A. Duncan, T. G. Dietz, and R. E. Smalley, *Chem. Phys.*, **44**, 415 (1979).
(2) D. P. Gerrity, L. J. Rothberg, and V. Vaida, *Chem. Phys. Lett.*, **74**, 1 (1980).
(3) G. J. Fisanick, T. S. Eichelberger, IV, N. A. Kuebler, and M. B. Robin, submitted for publication in *J. Chem. Phys.*
(4) P. M. Johnson, *Acc. Chem. Res.*, **13**, 20 (1980).
(5) L. J. Rothberg, D. P. Gerrity, and V. Vaida, submitted for publication in *J. Chem. Phys.*
(6) G. A. Junk and H. J. Svec, *Z. Naturforsch. B: Anorg. Chem., Org. Chem., Biochem., Biophys., Biol.*, **23B**, 1 (1968).
(7) H. M. Rosenstock, K. Draxl, B. W. Steiner, and J. T. Herron, *J. Phys. Chem. Ref. Data, Suppl.*, **6** (1977).

0020-1669/81/1320-3340$01.25/0

Table I. MPI Resonances in Hg Vapor

1-photon wavelength, Å	3-photon frequency, cm^{-1}	obsd 1-photon frequency[a]	assignt[a]
4207.9	71 295	71 295	6s → 7p
4147.5	72 333		
3902.9	76 866	76 863	6s → 8p
3884.1	77 238	77 241	6s → 5f

[a] From ref 10.

reported in the laser photolysis of ferrocene and nickelocene.[8] It is clear from the appearance potentials that very high photon numbers are involved in these nonlinear processes and from the mass spectra that the multiphoton paths to ionization are quite different from those active in electron-impact or single-photon ionizations.

The question naturally arises as to whether the unexpected nonlinear photochemical behavior of the carbonyls will carry over to other classes of metal organics. To this end, we have studied aspects of the MPI absorption, MPI mass, and electron-impact spectra of $Hg(CH_3)_2$, chosen as a prototype of metal alkyls. Were the nonlinear photochemistry of $Hg(CH_3)_2$ to parallel that of the carbonyls, the chain of events would be

$$Hg(CH_3)_2 \xrightarrow{x\hbar\nu} Hg + 2CH_3$$
$$\downarrow y\hbar\nu$$
$$Hg^* \xrightarrow{z\hbar\nu} Hg^+ + e^-$$

Taking a typical laser wavelength of 4000 Å, the first step would be a coherent two-photon absorption ($x = 2$) since the first excited state of $Hg(CH_3)_2$ is far above the energy of one photon, but very close to the energy of two photons. This absorption would be followed by dissociation to Hg(I). The excitation and ionization of the Hg(I) atom then requires another four photons with either $y = 2$, $z = 2$, or $y = 3$, $z = 1$. In the stepwise chain outlined above, the overall energy expenditure is 18.5 eV, whereas the one-photon appearance potential for Hg^+ from $Hg(CH_3)_2$ is only 13.05 eV.[9] This clearly illustrates one of the many differences between a multiphoton stepwise fragmentation/ionization of the sort given above and the more common one-photon process $Hg(CH_3)_2 \xrightarrow{1h\nu} Hg^+ + 2CH_3 + e^-$.

Support for the process having an Hg atom intermediate could come from two observations: (i) that the MPI spectrum of $Hg(CH_3)_2$ shows resonances at the characteristic Hg atom frequencies and (ii) that the MPI mass spectrum shows Hg^+ ions but no larger molecular species. At very low laser power, an I^6 power law for Hg^+ production also would be expected on the basis of $x = 2$ and $y + z = 4$, whereas the power exponent for Hg^+ production via $Hg(CH_3)_2^+$ would be 5, and for $Hg(CH_3)_2^+$ itself would be 3.

MPI Spectra. The search for Hg atom transitions in pulse-irradiated $Hg(CH_3)_2$ is simplified by first determining the MPI spectrum of Hg vapor. Use of a flat-plate cell biased at 190 V uncovered three identifiable lines in the 3600–4500-Å region (Table I). Each of these lines corresponds to a four-photon ionization, resonant at the third photon. A fourth line (4147.5 Å) has no complement in the previously observed one-photon spectrum of Hg[10] and is left unassigned.

The MPI spectrum of $Hg(CH_3)_2$ at room temperature is presented in Figure 1A. Searching the region 3540–5000 Å,

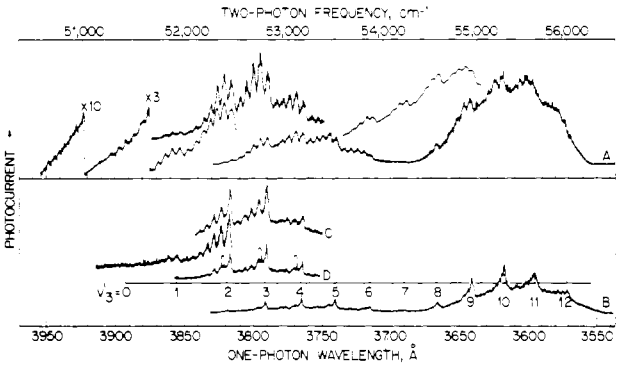

Figure 1. MPI spectrum of $Hg(CH_3)_2$ vapor (A) at room temperature and 2 torr and seeded in a supersonic expansion of Ar with a stagnation pressure between 400 and 600 torr (B–D). The degree of cooling was dependent upon the stagnation pressure and strongly on the point at which the laser beam crossed the jet.

no trace of a feature was found which could be assigned to any of the Hg transitions listed in Table I. Thus we have our first indication that MPI in $Hg(CH_3)_2$ does not follow a course paralleling that in the carbonyls. This is supported as well by the MPI mass spectrometric evidence presented below.

The most prominent feature in the MPI spectrum of $Hg(CH_3)_2$ is the long progression of 12 quanta of 350-cm^{-1} average spacing in the 3540–3900-Å one-photon region (Figure 1A). Other investigators[11] have observed one-photon transitions in the 2600–2100-Å region which also showed the 350-cm^{-1} interval and assigned it to the symmetric C–Hg–C stretch ν_3' (a_1, 515 cm^{-1} in the ground state[12]); we concur in this. Appended to each ν_3' ν_3' excitation are several intervals of approximately +60 cm^{-1}. These correspond to the $\Delta v = 0$ sequences stemming from the thermally populated ν_{11} C–Hg–C bending vibration (e', 161 cm^{-1} in the ground state). These sequences will be intense since, at room temperature, the population in $v = 1$ of ν_{11}'', for example, is 46% of that in $v = 0$. Nonetheless, all vibrational aspects of the band in question, sequences and progressions, are totally symmetric, and so we clearly are dealing with an allowed two-photon resonance.

Because the 60-cm^{-1} sequence interval roughly divides the 350-cm^{-1} vibrational interval into fifths, it is difficult in places to discern just which feature is the progression member and which is the sequence built upon it, i.e., the resonances look more like a regular parade of 60-cm^{-1} intervals. The problem is further compounded by the shift of relative intensity along the spectrum, so that, at one end, what appear to be progression members are most intense, whereas, at the other end of the spectrum, what appear to be sequences are most intense. This problem is solved by studying the MPI spectrum in a molecular beam formed by a jet-cooled expansion.[13] Depending upon the backing gas mixed with the absorber and the stagnation pressure, one is able to either cool the sample rotationally (thus sharpening the resonances and revealing splittings), cool the sample vibrationally (thus removing the sequences but leaving the progressions), and/or cluster other atoms or molecules about the absorber (thus testing the Rydberg/valence shell nature of the resonant state via perturbation of the band shape).[14]

The $Hg(CH_3)_2$ vapor above a liquid sample at 0 °C was mixed with approximately 1 atm of argon, and the mixture expanded cw through a 150-μm hole into the evacuated space

(8) S. Leutwyler, U. Even, and J. Jortner, *Chem. Phys. Lett.*, **74**, 11 (1980).
(9) G. Distefano and V. H. Dibeler, *Intn. J. Mass Spectrom. Ion Phys.*, **4**, 59 (1970).
(10) C. E. Moore, "Atomic Energy Levels", Vol. III, U.S. National Bureau of Standards, Washington, D.C., 1958, p 467.
(11) H. W. Thompson and J. W. Linnett, *Proc. R. Soc. London, Ser. A*, **156**, 108 (1936).
(12) T. Shimanouchi, *J. Phys. Chem. Ref. Data*, **6**, 993 (1977).
(13) A. Amirav, U. Even and J. Jortner, *Chem. Phys. Lett.*, **72**, 16 (1980).
(14) M. B. Robin, "Higher Excited States of Polyatomic Molecules", Vol. I, Academic Press, New York, 1974.

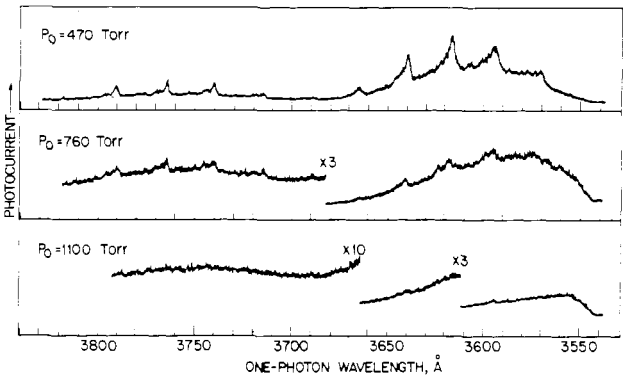

Figure 2. Clustering effects on the MPI spectrum of $Hg(CH_3)_2$ seeded into a supersonic expansion of Ar at stagnation pressure P_0.

between two parallel-plate electrodes biased at 200–250 V. The vacuum chamber was maintained below 0.1 torr by a 1560-l/min mechanical pump, while the laser light was focused between the plates and a few millimeters below the pinhole with a 50-mm lens. The N_2-pumped dye laser was operated with use of PBD/dioxane, PBD/ethanol–toluene, polyphenyl-1/ethylene glycol,[15] and BBQ/dioxane dye solutions.

As seen in Figure 1B, the expansion-cooled sample has an MPI spectrum which is free of almost all hot-band absorption, leaving only the ν_3' progression. The long-wavelength feature at 3893 Å (1946.5 Å in two photons) is admittedly weak, but reproducible, and is taken as the electronic origin. As regards sequences vs. progressions, the proper assignment of the ν_3' features is clear from the comparison of the room-temperature and cooled spectra (Figure 1, A and B). Note, however, that the 0–1 and 1–2 intervals are significantly larger (ca. 490 cm^{-1}) than those that follow (ca. 350 cm^{-1}), and we may be seeing two overlapped excitations in this region.

A number of interesting phenomena appear as the argon-backing pressure P_0 is varied. As illustrated in the 3750-Å region (Figure 1C), one can readily alter the populations so that the progression is stronger than the sequences as expected for vibrational cooling. At somewhat lower P_0, rotational cooling is achieved while still maintaining a sizeable (1,1) sequence intensity (Figure 1D). In this regime, each (1,1) sequence band is split into two components separated by 14 cm^{-1}, whereas the progression members are narrowed but not split. In Figure 2, the MPI spectra at higher P_0 are shown; the extreme cooling leads to the formation of $Hg(CH_3)_2$/Ar or more likely $[Hg(CH_3)_2]_n$ clusters[16] and a consequent washing out of the sharp-line spectrum.

One-Photon Spectrum. Because the inelastic electron scattering spectrum at 0° scattering angle and high incident energy is equivalent to the conventional absorption spectrum, we shall refer to it here as the "one-photon spectrum", even though the excitation does not involve photons. The electron impact spectrum in the 0–30-eV region shown in Figure 3 was obtained with use of a McPherson ESCA 14 spectrometer having a resolution of 0.015 eV (120 cm^{-1}) at 100.5-eV impact energy. As shown in the inset of Figure 3, two features are found in the wing of the elastic scattering peak, with energy losses of 2920 and 1194 cm^{-1}. These correspond to the ground-state vibrational excitation of ν_1 (a_1', 2911 cm^{-1}) and ν_2 (a_1', 1182 cm^{-1}), respectively.[12] Two excitations previously reported[11] in the optical spectrum of $Hg(CH_3)_2$ are seen here at 5.0–5.7 and 5.7 to beyond 6.1 eV; the bands beyond 6.5 eV are reported for the first time. Also shown in Figure 3, as

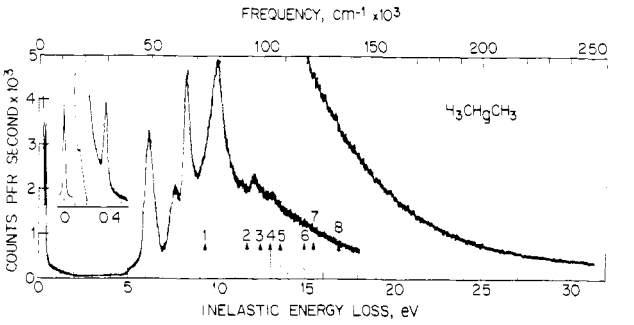

Figure 3. Electron-impact energy loss spectrum of $Hg(CH_3)_2$ taken at $\theta \approx 0°$ and an impact energy of 100.5 eV.

arrows, are the vertical ionization potentials reported by Eland[17] in the photoelectron spectrum of $Hg(CH_3)_2$. Note especially that the prominent two-photon resonance at 6.3–6.8 eV (Figure 1) is missing from the electron-impact spectrum, showing that it is two-photon allowed but one-photon forbidden.

MPI Mass Spectrum. A modified Bendix time-of-flight mass spectrometer was used together with ionizing pulses of 3546-Å tripled-YAG radiation. Ion flight times were digitized on a 10 ns/channel basis and the ion current accumulated in a CAT signal averager. Pressure in the mass spectrometer always was kept at 2×10^{-6} torr. Using soft focusing (50-cm lens) and low optical power (3 mJ) gave copious amounts of the ions CH_3^+, CH_3Hg^+, $(CH_3)_2Hg^+$, and Hg^+, whereas with tighter focusing (10-cm lens) and high power (30 mJ), only CH_3^+ and Hg^+ were observed. The power dependence of the mass-dispersed ion product yield is still under investigation, but it is clear that Hg^+ results from photofragmentation of $Hg(CH_3)_2^+$ and not from ionization of Hg(I). This is in accord with the MPI resonance spectrum result.

Further support for the proposition that the photoionization mechanism in $Hg(CH_3)_2$ involves ionization (possibly followed by fragmentation) rather than fragmentation followed by ionization is found in the power dependence of the ionization signal at low power (ca. 10^5–10^7 W/cm^2). If the primary ionization process is a (2 + 1) absorption to produce the parent ion, then the signal will vary as the cube of the incident optical power. On the other hand, fragmentation to Hg + $2CH_3$, followed by ionization of the Hg, will lead to a sixth-power dependence since $x + y + z = 6$. Working at 3806.6 Å in a flat-plate cell at 20 torr gave a power exponent of 3.0 at low power. The appearance potentials of the ionic fragments from $Hg(CH_3)_2$ have been reported by Distefano and Dibeler[9] as follows: CH_3Hg^+, 10.1; Hg^+, 13.05; CH_3^+, 12.55 eV (i.e., respectively 0.8, 3.75, and 3.52 eV above the ionization potential of 9.33 eV). With consideration of the width of the first photoelectron band, each of these thresholds is within one 3546-Å photon's energy of the ionic ground state and thus would be relevant in a (2 + 1 + 1) absorption scheme. Note that the parent ion does have an excited state 3.5 eV above its ground state[17] and that the transition to it is an allowed one.

Electronic Structure of $Hg(CH_3)_2$. The various spectroscopic observations discussed above can be rationalized in terms of the electronic structure of $Hg(CH_3)_2$. Though there is no calculation available on the electronic structure of this molecule, it can be sorted out in part from Eland's discussion of the photoelectron spectrum[17] and from the ground-state configuration of the Hg(I) atom ($1s^2...5p^65d^{10}6s^2$). The ionization potentials of $Hg(CH_3)_2$ are indicated by arrows in Figure 3 and are listed in Table II. Ionization potentials 6, 7, and 8 (14.95, 15.44, and 16.90 eV) originate in the 5d shell, which

(15) W. Hüsser, R. Schieder, H. Telle, R. Raue, and W. Brinkwerth, *Opt. Commun.*, **33**, 85 (1980).
(16) M. A. Duncan, T. G. Dietz, M. G. Liverman, and R. E. Smalley, submitted for publication in *J. Phys. Chem.*
(17) J. H. D. Eland, *Int. J. Mass Spectrom. Ion Phys.*, **4**, 37 (1970).

Table II. Spectral Assignments in $Hg(CH_3)_2$

excitation	intens[a]	IP	term value	assignt
42 750	w	75 250	32 500	$6p\sigma_+ \rightarrow 6p\pi(A_1' \rightarrow E''$ forbidden)
49 200	s	75 250	26 050	$6p\sigma_+ \rightarrow 6p\pi(A_1' \rightarrow E'$ allowed)
51 700	1-photon w, 2-photon s	75 250	23 550	$6p\sigma_+ \rightarrow 6p\pi(A_1' \rightarrow E''$ 2-photon allowed)
61 300	m, br	75 250	13 950	$6p\sigma_+ \rightarrow 6d$ (allowed)
		94 200	32 900	$6s\sigma_+ \rightarrow 6p\pi$(allowed)
66 140	s	75 250	9 110	$6p\sigma_+ \rightarrow 6d$ (allowed)
		101 000	34 860	MO6 $\rightarrow 6p\pi$ (allowed)
79 850	s	101 000	21 150	MO6 $\rightarrow 6p\pi$ (allowed)
		104 800	24 950	MO7 $\rightarrow 6p\pi$ (allowed)
		109 700	29 850	MO8 $\rightarrow 6p\pi$ (allowed)
91 500	m	120 600	29 100	$5d \rightarrow 6p\pi$ (allowed)
96 800	m	125 500	28 700	$5d \rightarrow 6p\pi$ (allowed)
104 800	m	136 300	31 500	$5d \rightarrow 6p\pi$ (allowed)

[a] Key: w = weak, s = strong, m = medium, br = broad.

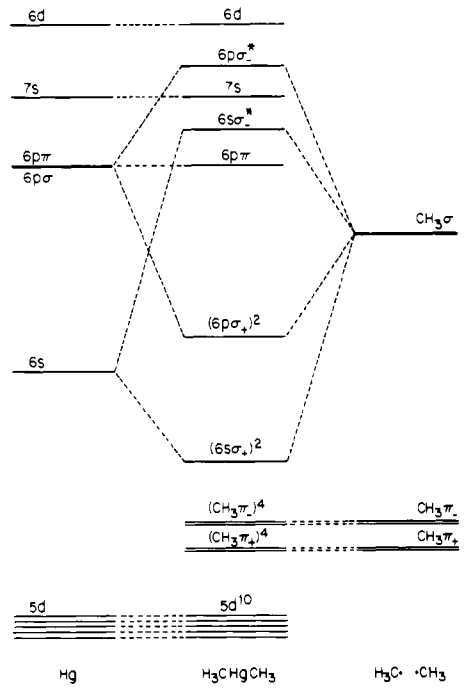

Figure 4. Qualitative ordering of the molecular orbitals of $Hg(CH_3)_2$ assembled from the group orbitals of two CH_3 fragments and the mercury atom AO's.

is split into five components by the strong spin–orbit coupling and by the axial ligand field; only three of the components are resolved. The uppermost filled orbital ($6p\sigma_+$, 9.33 eV) is a Hg–C bonding one involving the out-of-phase combination of carbon σ AO's and the otherwise vacant $6p\sigma$ Hg orbital (Figure 4).[17,18] The three remaining IP's in the 11–15-eV region encompass the π_+ and π_- orbitals of the CH_3 groups and $6s\sigma_+$, an MO in which the Hg 6s level is stabilized through a bonding interaction with the in-phase combination of CH_3 group σ orbitals. Actually, four bands are observed between 11 and 15 eV in the photoelectron spectrum (11.68, 12.52, 13.0, and 13.6 eV), and one must further assume that either the $^2\Pi_+$ or $^2\Pi_-$ state is Jahn–Teller split. The 11.68-eV band is far too low for a CH_3 group ionization and must correspond to the $6s\sigma_+$ orbital in question.

From a look at the virtual MO's, it is clear that $6p\pi$ is relatively nonbonding and hence will be lower than 7s, $6p\sigma_-$*, and 6d (Figure 4). The location of the $6s\sigma_-$* MO is unknown, as is the relative ordering of 7s and $6p\sigma_-$*; the 6d Rydberg orbital will be about 1 eV above 7s.

The simple one-electron scheme depicted in Figure 4 will be upset considerably by the intense spin–orbit coupling at the Hg atom. In the lowest excited configuration $(6p\sigma_+)^1(6p\pi)^1$, one has a situation much like that in the lowest Rydberg excited state of CF_3I,[19] and the analyses are parallel. In $Hg(CH_3)_2$, the $(6p\sigma_+)^1$ and $(6p\pi)^1$ spin orbitals transform as $E_{5/2}$ and $E_{3/2}$, $E_{5/2}$, respectively, and the two-electron configuration generates representations given by their direct product, i.e., E'', E', A_2', A_1', and E''. In D_{3h} symmetry, excitations from the ground state will be allowed in one-photon only to E' of the above. The $(6p\sigma_+)^1(6s\sigma_-^*)^1$ and $(6p\sigma_+)^1(7s)^1$ configurations will split into A_1'', A_2'', and E' spin–orbit states, while $(6p\sigma_+)^1(6p\sigma_-^*)^1$ yields A_1', A_2', and E_2''.

Term Values and Assignments. In saturated molecules such as $Hg(CH_3)_2$, most if not all of the discrete absorption can be assigned to excitations from the few highest occupied MO's to the lowest molecular Rydberg levels of symmetry (or near-symmetry) s, p, and d. The separations of these Rydberg levels from the appropriate ionization potentials, called term values, are often used as diagnostics for the symmetries of the Rydberg orbitals in nonmetal-containing molecules.[14] In the case of $Hg(CH_3)_2$, it is not altogether clear what to expect; however, the term values of Hg itself offer a reasonable starting point for discussion. The energy of the 6p orbital of Hg(I) fits nicely into the $6s^1np^1$ atomic singlet Rydberg series,[10] and so the $6p\pi$ virtual orbital of $Hg(CH_3)_2$ undoubtedly will be strongly Rydberg in character, though a small amount of $CH_3\pi_+$ valence character also may be present. In the atom, the 6p term value is 30 115 cm^{-1}. By contrast, 6s becomes a part of the valence shell in $Hg(CH_3)_2$, and because $6s\sigma_-$* is then an antibonding valence orbital rather than Rydberg, transitions to it will not follow any simple term value expectations. Most often, valence-shell excitations in saturated molecules appear as broad continua of uncertain energy and intensity underlying the sharper Rydberg excitations.[14] Molecular excitations to 7s and 6d orbitals are outside the valence shell and will have term values close to those of the atom (20 256 and 12 851 cm^{-1}, respectively).

With the use of the term value concepts given above and the one-photon and two-photon selection rules, all of the discrete transitions in $Hg(CH_3)_2$ can be assigned as Rydberg excitations (Table II). As anticipated, the valence excitations to $6s\sigma_-$* are not seen explicitely but presumably are part of the underlying continuum in the region beyond 7 eV.

The weak one-photon excitation at 42 750 cm^{-1} (Figure 3) is assigned as the $A_1' \rightarrow E''$ forbidden component of the $6p\sigma_+$ $(a_2'') \rightarrow 6p\pi$ (e') promotion, with a term value (32 500 cm^{-1}) close to that of the 6p term value of the Hg atom (30 115 cm^{-1}). The strong band at 49 200 cm^{-1} then follows naturally as the $A_1' \rightarrow E'$ one-photon allowed excitation from $6p\sigma_+$ to $6p\pi$.

The MPI excitation at 51 700 cm^{-1}, being two-photon allowed and one-photon forbidden, is compatible with each of the three remaining $6p\sigma_+ \rightarrow 6p\pi$ transitions $A_1' \rightarrow A_2'$, A_1', and E''. The ambiguity in assignment can be resolved by referral to the cold spectrum of Figure 1D. The observation that in the rotationally-narrowed spectrum the (1,1) ν_{11} sequence band is split by 14 cm^{-1} while the progressions are narrowed but not split parallels an example of Jahn–Teller splitting in CF_3I discussed by Herzberg.[19] In the case of an upper-state electronic degeneracy (e.g., E''), the simultaneous excitation of a degenerate vibration (say, ν_{11}'e') then leads to an E'' X E' factoring of the vibronic level into A_1'', A_2'', and

(18) T. P. Fehlner, J. Ulman, W. A. Nugent, and J. K. Kochi, *Inorg. Chem.*, **15**, 2544 (1976).

(19) G. Herzberg, "Molecular Spectra and Molecular Structure", Vol. III, Van Nostrand-Reinhold, New York, 1966.

E″ components, with two-photon excitations allowed to the last two of these. Because the splitting cannot arise in excitations to the electronic A_2' or A_1' states, we take its presence as strong evidence for an E″ upper state. Note also that this splitting will not be observed in vibronic components lacking e′ vibrational excitation (say ν_3' progressions), just as observed in Figure 1D. Splitting in the (2,2) and higher sequences also is predicted, but the vibrational Boltzmann factors are too small at low temperature for the splittings to be seen.

In a two-photon-allowed $A_1' \rightarrow E''$ excitation, both E′ and A_2'' states can act as one-photon intermediates. The nearby E′ level at 49 200 cm^{-1} would seem to be especially well suited for this. Note also that the appearance of identical vibrational structures in the 42 750-, 49 200-, and 51 700-cm^{-1} bands of $Hg(CH_3)_2$ follows naturally from the fact that they have the ($6p\sigma_+$, $6p\pi$) parentage in common. The simplicity of this vibronic progression shows that the only geometric change induced by promoting an electron from $6p\sigma_+$ to $6p\pi$ is to lengthen the Hg–C bonds in the upper states while maintaining D_{3h} symmetry.

Whereas it is only assumed that the excitations at 42 750 and 49 200 cm^{-1} terminate at Rydberg levels, this assumption for the 51 700-cm^{-1} band can be tested experimentally. It is well-known that valence-shell excitations in matrices will be very sharp (if they are not continuous), whereas Rydberg excitations in the same situation are greatly broadened.[14] We have found that this test can be most easily applied in the MPI spectrum by clustering, with the use of either N_2 or Ar as carrier gas in the jet expansion. Applying this concept to the 51 700-cm^{-1} band of $Hg(CH_3)_2$ (Figure 2), one concludes that the broadening on cluster formation is that characteristic of a Rydberg upper state. In contrast to this, we have observed that valence-shell excitations within clusters show the sharp zero-phonon lines and phonon side bands characteristic of valence excitations in matrices.

As for the missing $A_1' \rightarrow A_1'$ and A_2' components of the $6p\sigma_+ \rightarrow 6p\pi$ excitation, they are both one-photon forbidden but two-photon allowed. An irregular series of weak bands is observed in the 2180–2040-Å two-photon region of the MPI spectrum and may be due to one of the above excitations or possibly to the $A_1' \rightarrow E'$ transition already observed in this region of the one-photon spectrum.[11]

It is clear from the analysis so far that each of the other one-electron excitations (Figure 4) will give rise to its own set of spin–orbit components of large splitting and that the data of Figure 3 are far too meager to allow sorting these out with confidence. Nonetheless, the term values observed for $6p\sigma_+ \rightarrow 6p\pi$ excitations (32 500, 26 050, and 23 550 cm^{-1}) reappear often, along with that expected for excitation to 6d (Table II) and allow a consistent but not necessarily unique assignment of the remainder of the one-photon spectrum. Excitations from the three 5d levels to $6p\pi$ are one-photon allowed (a_1', e′, e″ → e′) and are observed to have term values of 30 000 ± 1000 cm^{-1}. Though allowed, these excitations are weak for reasons of poor overlap between the 5d AO and the $6p\pi$ MO. It is especially interesting to note that the lowest Rydberg orbital in $Hg(CH_3)_2$ is not s type, in contrast to the situation in hydrocarbons, and that the lowest p-type orbital assumes a term value much larger than that in the hydrocarbons. This increase is due in part to the fact that in such a heavy-atom molecule as $Hg(CH_3)_2$ spin–orbit coupling intensifies absorption by Rydberg triplets which necessarily have larger term values than the corresponding singlets of hydrocarbons.

What then about M^+ production in the metal alkyls? The key to the phenomenon in carbonyls is that the excited states are very rapidly dissociated as evidenced by the extreme widths of their absorption bands. This dissociation is faster than photon ladder climbing so that atomic fragments are produced rather than molecular ions. Clearly, then, the sharp-line nature of the lowest absorptions in $Hg(CH_3)_2$ implies excited-state molecular stability, and so molecular ions are observed as the primary ionic fragments; M^+ is obtained only by further absorption by and fragmentation of the parent ion. We note, however, that there are other metal alkyls such as $Pb(C_2H_5)_4$ and $Sn(CH_3)_4$ with encouragingly broad spectra,[11] and perhaps these will more closely follow the behavior of carbonyls. This work is now under way.

Acknowledgment. Several discussions with Robert Gooden are gratefully acknowledged, as well as the expertise of William R. Harshbarger in obtaining the electron impact spectra. We thank R. E. Smalley for a preprint of his work on spectra in molecular beams.

Registry No. $Hg(CH_3)_2$, 593-74-8.